Gorazd ŠTUMBERGER[1,2], Željko PLANTIĆ[2], Bojan ŠTUMBERGER[1,2], Tine MARČIČ[2]

University of Maribor (1), TECES - Research and Development Centre of Electrical Machines (2)

Impact of static and dynamic inductance on calculated time responses

Abstract. *This paper focuses on electromagnetic devices and electric machines with magnetic cores. Their behavior is magnetically nonlinear. In magnetically nonlinear dynamic models of these devices, the magnetically nonlinear behavior can be accounted for by the characteristics flux linkages versus magneto-motive-force or by the current dependent dynamic and static inductances. This paper discusses different methods for determining characteristics of flux linkages and the impact of static and dynamic inductances on calculated dynamic responses.*

Streszczenie. *W artykule skoncentrowano się na urządzeniach i maszynach elektrycznych z rdzeniem magnetycznym. Praca tych urządzeń wykazuje się magnetyczną nieliniowością. W nieliniowych magnetycznie dynamicznych modelach tych urządzeń uwzględnia się fakt nieliniowości poprzez wstawianie zależności strumienia magnetycznego od siły magnetomotorycznej (przepływu) lub poprzez przyjmowanie dynamicznych i statycznych indukcyjności. Artykuł przedstawia dyskusję różnych metod określania zarówno zależności wspomnianej, jak i wpływu dynamicznych i staycznych indukcyjności na dynamiczne odpowiedzi. (**Wpływ statycznej i dynamicznej indukcyjności na obliczane odpowiedzi czasowe**)*

Keywords: magnetic cores, devices, static inductance, dynamic inductance.
Słowa kluczowe: rdzenie magnetyczne, urządzenia, statyczna indukcyjność, dynamiczna indukcyjność

Introduction

Magnetic cores of different electromagnetic devices and electric machines are normally made of ferromagnetic materials. These materials have magnetically nonlinear characteristics, which imply that the electromagnetic devices and machines made of these materials behave magnetically nonlinearly as well. Nowadays, there exist many software packages developed for computation of electric power system transients and dynamic evaluation of electric drives, electric machines and electromagnetic devices. In order to improve agreement between measured and calculated responses, dynamic models of electric machines and electromagnetic devices used in these software packages have to be completed by magnetically nonlinear models of magnetic cores.

The magnetically nonlinear behavior of magnetic material is often described in the form of magnetic field strength H dependent magnetic field density B, known as $B(H)$ characteristic [1]. The ratio between the magnetic flux density and magnetic field strength is called permeability, while the slope of $B(H)$ characteristic is called dynamic permeability. Although the magnetic cores are composed of magnetic material, the magnetically nonlinear behavior of the entire electromagnetic devices is normally described in the form of current i dependent characteristics of flux linkages $\psi(i)$. They can be determined from currents and voltages measured on the device terminals during different tests. In [2] Calabro explained that the measurement of root mean square (RMS) values of currents and voltages on device terminals is insufficient for proper determination of flux linkage characteristics. The ratio between the flux linkage and current and the slope of $\psi(i)$ characteristic are applied to define the static and dynamic inductances in [3].

In the case of magnetically anisotropic material, its magnetically nonlinear behavior is described by the permeability tensor [1]. Similarly, the magnetically nonlinear and anisotropic behavior of magnetic cores in electromagnetic devices and electric machines can be described by current dependent characteristics of flux linkages and their partial derivatives, where only independent variables can be used [4]-[6]. Some of the methods appropriate for determining current dependent flux linkage characteristics of electromagnetic devices and electric machines are shown in [7] and [8].

This paper focuses on two fields. The first one is related to the methods for determining current dependent flux linkage characteristics, which are used to describe magnetically nonlinear behavior of electromagnetic devices and electric machines. The second one is related to the use of current dependent static and dynamic inductances in dynamic models. The paper shows the impact of improperly considered waveforms of measured currents on determined current dependent characteristics of flux linkages. These characteristics are applied to determine static and dynamic inductances. Since both inductances are current dependent, the static inductance is often misused in calculation of dynamic responses. In the case study, the paper shows differences between calculated current responses in the cases when current dependent static and dynamic inductances are used in the dynamic model of a simple iron core inductor.

Determining current dependent characteristics of flux linkages

In [2] the authors reported that actual waveforms of measured currents and voltages should be used to determine realistic magnetically nonlinear characteristics of magnetic cores, which are substantial parts of transformers and iron core inductors. However, almost 25 years later, characteristics of iron core inductors and transformers installed in distribution networks are in the best case available in the form of measured power and RMS values of currents and voltages. These values, normally given for no-load test, are used to determine magnetically nonlinear characteristics of magnetic cores, required in dynamic models of these devices.

The iron core inductor is the simplest electromagnetic device with magnetic core. It will be used as a test object in this paper. The waveforms of currents and voltages measured on its terminals are substantial for proper determination of current dependent flux linkage characteristics, which are used to describe magnetically nonlinear behavior of the magnetic core. Neglecting losses in the magnetic core, the voltage balance can be described by (1):

$$u = Ri + \frac{d\psi}{dt} \tag{1}$$

where u is the applied voltage, i is the current, R is the resistance, while ψ denotes the flux linkage. Fig. 1 shows waveforms of voltage and current measured at the terminals of the test inductor during no-load operation. They are given together with their amplitude spectra.

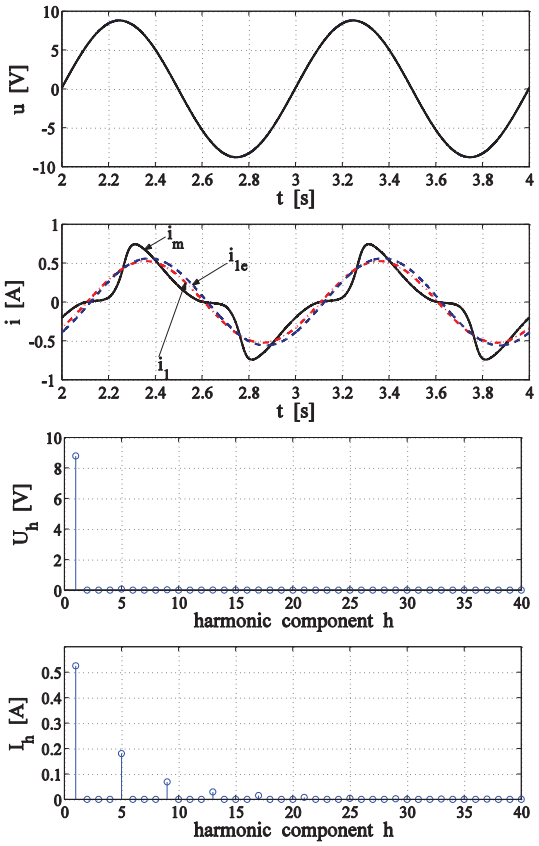

Fig.1. Voltage u and current i_m measured at the terminals of iron core inductor, current fundamental harmonic component i_1 and equivalent fundamental harmonic component current i_{1e}, and voltage and current amplitude spectra U_h and I_h, given as functions of harmonic component h

The measured voltage and current shown in Fig.1 are periodical functions. The voltage contains exclusively fundamental harmonic component, while the current contains also higher order harmonic components. The waveforms of the h-th harmonic order voltage $u_h(t)$ and current $i_h(t)$ can be described by (2), as functions of the time t:

$$\begin{aligned} u_h(t) &= a_{hu}\cos(h\omega t) + b_{hu}\sin(h\omega t) = U_h\cos(h\omega t - \varphi_{hu}) \\ i_h(t) &= a_{hi}\cos(h\omega t) + b_{hi}\sin(h\omega t) = I_h\cos(h\omega t - \varphi_{hi}) \end{aligned} \tag{2}$$

where a_{hu}, b_{hu}, and a_{hi}, b_{hi} are the Fourier coefficients, U_h and I_h are the voltage and current amplitudes of the harmonic order h, φ_{hu} and φ_{hi} are the voltage and current phase angles of the harmonic order h, u and i are the measured voltage and current, T denotes one cycle of the fundamental frequency, $\omega=2\pi/T$ is the fundamental angular frequency, while τ the auxiliary integration variable in (3).

$$\begin{aligned} a_{hu} &= \frac{2}{T}\int_0^T u(\tau)\cos(h\omega\tau)d\tau, \quad b_{hu} = \frac{2}{T}\int_0^T u(\tau)\sin(h\omega\tau)d\tau \\ a_{hi} &= \frac{2}{T}\int_0^T i(\tau)\cos(h\omega\tau)d\tau, \quad b_{hi} = \frac{2}{T}\int_0^T i(\tau)\sin(h\omega\tau)d\tau \\ U_h &= \sqrt{a_{hu}^2 + b_{hu}^2}, \quad \varphi_{hu} = \arctan\frac{b_{hu}}{a_{hu}} \\ I_h &= \sqrt{a_{hi}^2 + b_{hi}^2}, \quad \varphi_{hi} = \arctan\frac{b_{hi}}{a_{hi}} \end{aligned} \tag{3}$$

For each harmonic order h, the impedance Z_h and active power P_h are defined by (4):

$$Z_h = \frac{U_h}{I_h}, \quad P_h = \frac{U_h}{\sqrt{2}}\frac{I_h}{\sqrt{2}}\cos(\varphi_h) \tag{4}$$

where φ_h is the phase angle of the harmonic order h. The total active power P and the RMS values of voltage U_{RMS} and current I_{RMS} are given by (5):

$$\begin{aligned} P &= \frac{1}{T}\int_0^T u(\tau)i(\tau)d\tau \\ U_{RMS} &= \sqrt{\frac{1}{T}\int_0^T u^2(\tau)d\tau}, \quad I_{RMS} = \sqrt{\frac{1}{T}\int_0^T i^2(\tau)d\tau} \end{aligned} \tag{5}$$

Let us consider exclusively the fundamental harmonic components of voltage and current. After applying (3) and (2) on the measured voltage and current for h=1, the voltage and current fundamental harmonic components waveforms $u_1(t)$ = $u(t)$ and $i_1(t)$, shown in Fig. 1, are obtained. Consequently, the voltage and current amplitudes U_1 and I_1 are obtained by (3), while the impedance Z_1 and active power P_1 are obtained by (4). The resistance R_1, inductance L_1 and flux linkage $\psi(I_1)$ are calculated by (6), considering exclusively the fundamental harmonic components of the measured voltage and current.

$$R_1 = \frac{P_1}{\left(I_1/\sqrt{2}\right)^2}, \quad L_1 = \frac{1}{\omega}\sqrt{Z_1^2 - R_1^2}, \quad \psi(I_1) = L_1 I_1 \tag{6}$$

To determine the $\psi(I_1)$ characteristic over entire range of operation, different amplitudes of the voltage shown in Fig. 1 must be applied.

Let us explain how the equivalent fundamental harmonic voltage, current and phase angle are often defined. Instead to measure the actual waveforms of voltage and current, the active power P and RMS values of voltage U_{RMS} and current I_{RMS} defined by (5), are measured directly by instruments. In this way, the information related to the harmonic contents, shown in Fig. 1, is lost. The measured RMS values are treated as fundamental harmonic component. Therefore, the corresponding values are marked with indices $1e$. In this way, the so called equivalent fundamental harmonic component voltage, current and phase angle are defined (7):

$$I_{1e} = I_{RMS}\sqrt{2}, \quad U_{1e} = U_{RMS}\sqrt{2}, \quad \arccos(\varphi_{1e}) = \frac{P}{I_{RMS}U_{RMS}} \tag{7}$$

Since the measured voltage u, shown in Fig. 1, contains only fundamental harmonic component, U_{1e} equals U_1. Considering this, I_{1e} and φ_{1e} can be used in (3) and (2) to determine waveform of equivalent fundamental harmonic component current $i_{1e}(t)$, shown in Fig. 1. By replacing P_1 and I_1 in (6) with I_{1e} and P from (7), expressions (6) can be used to determine flux linkage for equivalent fundamental harmonic component current $\psi(I_{1e})$. Again, to determine the flux linkage characteristic over entire range of operation, different amplitudes of voltage shown in Fig. 1 must be applied.

Finally, the $\psi(i)$ characteristic can be determined also considering the actual waveforms of the measured voltage and current shown in Fig. 1. One of the possible solutions is numerical integration (8):

(8) $$\psi(t) = \int_0^t [u(\tau) - Ri(\tau)]d\tau + \psi(0)$$

where $u(t)$ and $i(t)$ are the waveforms of the measured voltage and current, R is the resistance, $\psi(0)$ is the integration constant due to the remanent flux, while $\psi(t)$ is the flux linkage waveform. The flux linkage $\psi(t)$ can be represented as a function of $i(t)$ in the form of a hysteresis loop $\psi(i)$. Considering only end points of each hysteresis loop, determined for different amplitudes of applied voltage $u(t)$, shown in Fig. 1, a unique current dependent flux linkage characteristic $\psi(i)$ is obtained. Detailed descriptions are given in [5],[7] and [8].

Fig. 1 shows actual waveform of the measured current $i_m(t)$, its approximation with the fundamental harmonic component $i_1(t)$ and approximation with the equivalent fundamental harmonic component current $i_{1e}(t)$. The corresponding characteristics $\psi(i)$ are shown in Fig. 2.

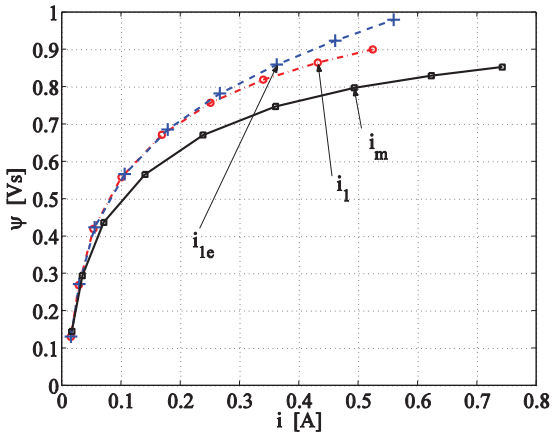

Fig.2. Current dependent characteristics $\psi(i)$ determined for currents i_m, i_1 and i_{1e} shown in Fig.1

The results presented in Fig. 1 clearly show that the peak values of $i_1(t)$ and $i_{1e}(t)$ are too small due to the neglected higher order harmonic components. Consequently, the $\psi(i)$ characteristics, determined for $i_1(t)$ and $i_{1e}(t)$ and shown in Fig. 2, have too high values. This results in too small values of calculated currents during switch-on of the inductors and transformers in the cases when $\psi(i)$ characteristics determined with $i_1(t)$ and $i_{1e}(t)$ are used in the dynamic models [9].

Static and dynamic inductances and their impact on calculated time responses

The previous section shows how the $\psi(i)$ characteristic can be determined properly. This section deals with the current dependent static inductance $L(i)$ and dynamic inductance $L_d(i)$. They are normally determined from known $\psi(i)$ characteristic by (9).

(9) $$L(i) = \frac{\psi(i)}{i}, \quad L_d(i) = \frac{\partial\psi(i)}{\partial i}$$

Fig. 3 shows characteristics $\psi(i)$, $L(i)$ and $L_d(i)$.

Considering (9), (1) can be expressed in the forms (10) and (11).

(10) $$u = Ri + \frac{d\psi(i)}{dt} = Ri + \frac{\partial\psi(i)}{\partial i}\frac{di}{dt} = Ri + L_d(i)\frac{di}{dt}$$

(11) $$u = Ri + \frac{d\{L(i)i\}}{dt}$$
$$u = Ri + \frac{d\{L(i)\}}{dt}i + L(i)\frac{di}{dt} = Ri + \frac{\partial\{L(i)\}}{\partial i}\frac{di}{dt}i + L(i)\frac{di}{dt}$$

In the case of magnetically linear circuits, the ratio between the inductance L and resistance R is used to define the time constant. However, in the case of magnetically nonlinear circuits the ratio between the dynamic inductance L_d and resistance R can be used only to determine local speed of current changes. Since the static and dynamic inductances are current dependent, the static inductance L is often used in (10) instead of dynamic inductance L_d, which means that the term with partial derivative in (11) is neglected. Fig. 4 shows applied voltages and currents calculated using (10) and (11), where partial derivative in (11) is neglected.

The results presented in Fig. 4 clearly show substantial differences between currents calculated with static and dynamic inductances. According to the waveforms of calculated currents it can be assumed that even in some recently published papers magnetically nonlinear behavior of magnetic cores could be accounted for improperly.

Conclusion

In the case study, the paper deals with two problems related to the proper use of magnetically nonlinear dynamic models of electromagnetic devices and electric machines. It is shown, that the magnetically nonlinear behavior of magnetic cores can be accounted for properly, in the form of current dependent flux linkage characteristics, only when actual waveforms of measured voltages and currents are considered. Although both, the static and dynamic inductances are current dependent, only their proper use can lead to the correct results.

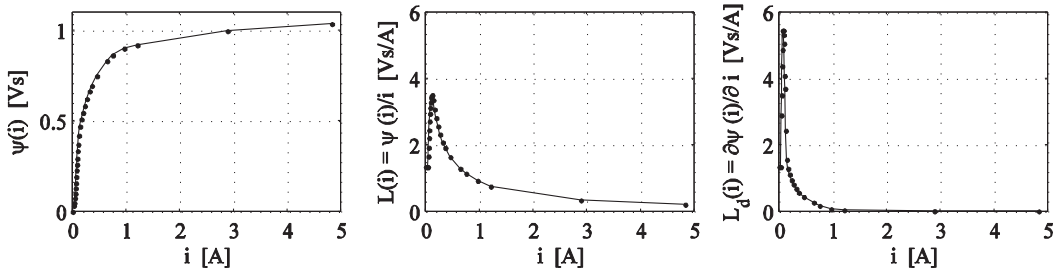

Fig.3. Current dependent characteristic $\psi(i)$, static inductance $L(i)$ and dynamic inductance $L_d(i)$

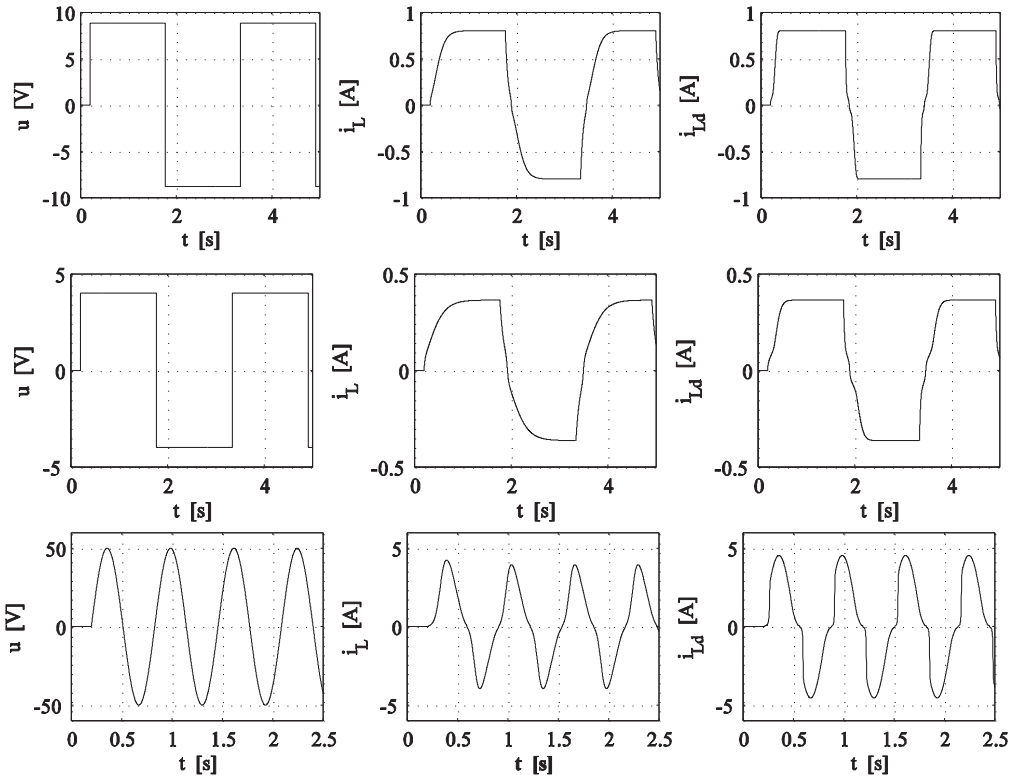

Fig.4. Applied voltage u and currents calculated using static inductance i_L and dynamic inductance i_{Ld}

Acknowledgments: This work was partly supported by the Slovenian Research Agency (ARRS), project no. L2-2060 and P2-0115.

REFERENCES

[1] Boll R., *Weichmagnetische Werkstoffe*, Vakuumschmelze GmbH, 1990

[2] Calabro S., Coppadoro F., and Crepaz S., "The measurement of the magnetization characteristics of large power transformers and reactors through d.c. excitation", *IEEE Transactions on Power Delivery*, 1 (1986), No. 4, 224-232

[3] Ganji A., Guillaume P., Pintelon R. and Lataire P., "Induction motor dynamic and static inductance identification using a broadband excitation technique", *IEEE Transactions on Energy Conversion*, 13 (1998), No. 1, 15-20

[4] Štumberger B., Štumberger G., Dolinar D., Hamler A., Trlep M., "Evaluation of Saturation and Cross-Magnetization Effects in Interior Permanent-Magnet Synchronous Motor", *IEEE Transactions on Industry Applications*, 39 (2003), No. 5, 1264-1271

[5] Štumberger G., Štumberger B. and Dolinar D., "Identification of linear synchronous reluctance motor parameters", *IEEE Transactions on Industry Applications*, 40 (2004), No. 5, 1317-1324

[6] Hadžiselimović M., Štumberger G., Štumberger B., Zagradišnik I., "Modeling of permanent magnet synchronous motor in d-q coordinates*", Prz. Elektrotech*, (2005) 81, No. 12, 38-40

[7] Štumberger G., Polajžer B., Štumberger B., Toman M. and Dolinar D., "Evaluation of experimental methods for determining the magnetically nonlinear characteristics of electromagnetic devices*", IEEE Transactions on Magnetics*, 41 (2005), No. 10, 4030-4032

[8] Štumberger G., Marčič T., Štumberger B. and Dolinar D., "Experimental method for determining magnetically nonlinear characteristics of electric machines with magnetically nonlinear and anisotropic iron core, damping windings, and permanent magnets", *IEEE Transactions on Magnetics*, (2008) 44, No. 11, 4341-4344

[9] Štumberger G., Seme S., Deželak K., Polajžer B., Toman M. and Dolinar D., "The impact of magnetically nonlinear iron core characteristics on responses of three-phase power transformer dynamic model", Proceedings XII International Symposium on Electromagnetic Fields in Mechatronics, Electrical and Electronic Engineering, 15-17 September, 2005, Baiona, Spain, f. 6

***Authors**: prof. dr. Gorazd Štumberger, and doc. dr. Bojan Štumberger, University of Maribor, Faculty of Electrical Engineering and Computer Science, Smetanova 17, 2000 Maribor, Slovenia, E-mail: gorazd.stumberger@uni-mb.si, bojan.stumberger@uni-mb.si, Željko Plantić and dr. Tine Marčič, TECES - Research and Development Centre of Electrical Machines, Pobreška cesta 20, 2000 Maribor, Slovenia, E-mail: zeljko.plantic@teces.si, tine.marcic@teces.si.*